

## Ti:LiNbO<sub>3</sub> 2×2 Optical Add/Drop Multiplexers Utilizing Acousto-Optic Effect

Gi-Jo Jung, Jung-Hee Kim, and Hong-Sik Jung\*

*Dept. of Electronic and Computer Engineering,  
Graduate School Hong-Ik University, Chochiwon 339-701, KOREA*

(Received December 31, 2001)

An integrated optical 2×2 add/drop multiplexer in X-cut, Y-propagating LiNbO<sub>3</sub> has been demonstrated. The device consists of passive polarization splitters and acousto-optical mode converters with weighted coupling utilizing tapered acoustical directional couplers; their specific design and properties are discussed. The insertion loss has been measured to be about -8.16 dB and -8.6 dB for TE and TM polarizations, respectively. The device shows a 3 dB bandwidth of 2.3 nm, a tuning rate 8.34 nm/MHz around  $\lambda = 1554$  nm, and a sidelobe suppression of about 14.5 dB. Optimum operation is achieved with a RF drive power of about 43 mW. Multi-wavelength operation has been demonstrated.

*OCIS codes* : 130.0130, 130.2790, 130.3060, 130.3120, 130.3730.

### I. INTRODUCTION

Optical networks are becoming a reality as the physical layer of high-performance telecommunication networks. The deployment of wavelength-division multiplexing (WDM) technology allows the full exploitation of the already installed fibers now facing an increasing traffic capacity demand. The routing of channels at the optical level and the insertion/extraction of channels in/from WDM aggregates, without preventing the transparent transit of throughput traffic, are key functions to ensure networking capabilities, support advanced protection and restoration schemes, and deploy a general-purpose platform for several types of clients [1].

Therefore, much effort is being made to find methods of manipulating multiple wavelengths to achieve high performance WDM systems. The optical add/drop multiplexer (OADM), which adds and drops optical signals on a transmission line, performs the most basic functions of WDM networks [2]. In the ring architecture, an OADM can be introduced to make efficient use of network capacity, network protection, wavelength routing, and many more features. In addition, photonic networks based on OADMs will provide openness and transparency in future networks to accommodate various client signals with different bit rates and formats (e.g., SONET, SDH, ATM, and IP) efficiently and forward the client signals transparently

to end users [3,4].

OADMs have been constructed in many ways. Guided-wave electro-optic tuned filters (EOTF) [5] and strain-optic tuned filters (SOTF) [6] have been produced in lithium niobate and lithium tantalate using polarization-selective directional couplers in a Mach-Zehnder configuration. The EOTF required separate voltage controls for the directional couplers, phase-matched polarization converters, and wavelength tuning sections, so the device was somewhat complex and inefficient in the use of the available length of the substrate. The SOTF utilized the static strain optic effect from a spatially periodic surface film. The device, however, showed very narrow tuning range and required very high tuning voltage.

In this paper, we report a LiNbO<sub>3</sub> waveguide-type acousto-optic OADM which has many excellent characteristics, for example, simultaneous multi-wavelength selection, a broad tunable bandwidth of more than 100 nm, and direct wavelength selection without scanning. In section II, the operational principle and properties of the single components required to form the OADM are discussed. Section III describes the design and fabrication. The device performance is presented and discussed in section IV.

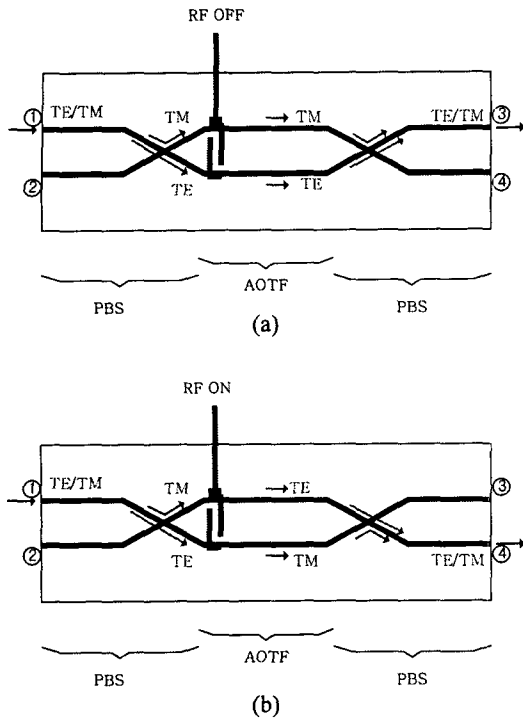


FIG. 1. Schematic diagrams illustrating operation principle of OADM (a) without SAW and (b) with SAW.

## II. DEVICE DESIGN AND PRINCIPLE OF OPERATION

A schematic diagram of OADM is shown in Fig. 1. The device consists of two polarization splitters and two acousto-optical mode converters. The incoming optical signal is split into two parts according to its polarization components by the first polarization splitter. TM polarized waves are routed to the bar state, TE polarized waves to the cross-state output of the polarization splitter. Assuming a signal entering at input port 1 the TM and TE components are directed toward the upper and lower mode converter, respectively. Within each mode converter the state of polarization can be converted from TE to TM or vice versa. Behind the mode converters the two branches are recombined within a second polarization splitter. If no mode conversion takes place, each polarization component of the input signal is passing both polarization splitters in the same manner. Therefore, the input signal is routed toward the output 3 of the device as shown in Fig. 1(a). The device is in the bar-state. If mode conversion takes place at the wavelength of the input signal, the TM(TE) polarized wave entering the upper(lower) mode converter is TE(TM) polarized. Thus, the converted signal is routed toward output 4 when passing the second polarization splitter. The device is in the cross-state as shown in Fig. 1(b) [7].

The optical waveguides are embedded in a common acoustical waveguide which forms one branch of an acoustical directional coupler. In the other branch, a surface acoustic wave (SAW) can be excited via an RF signal applied to the interdigital transducer (IDT) electrodes. The SAW is coupled to the adjacent acoustical guide and back again resulting in a weighted acousto-optical interaction [8,9]. This yields a wavelength dependent coupling between TE and TM polarized optical modes, if the phase-matching condition is fulfilled:

$$|\beta_{TE} - \beta_{TM}| = K_{ac} \quad (1)$$

with  $\beta_{TE}$  and  $\beta_{TM}$  being the wavenumbers of the optical TE- and TM-polarized wave, respectively, and  $K_{ac}$  being the wavenumber of the SAW. As  $\Delta\beta = \beta_{TE} - \beta_{TM}$  varies with the optical wavelength  $\lambda$ , a wavelength-selective TE/TM conversion is achieved, if  $K_{ac}$  is given by a SAW of a specific frequency. The phase-matched wavelength  $\lambda_0$  can now be tuned by changing the SAW frequency  $f_{ac}$  [10].

By applying a set acoustical frequencies at the transducer electrodes, a simultaneous filtering of different wavelengths is possible. Additionally, the TE/TM conversion efficiency can be controlled by adjusting the SAW power, which allows a defined attenuation of the filtered optical modes. These two properties make the AOTF particularly interesting for WDM network applications as they might help to decrease the number of components needed in node.

## III. COMPONENT DESIGN AND FABRICATION

### 1. Optical and Acoustical Waveguides

As substrate materials X-cut  $\text{LiNbO}_3$  with Y-propagation is used. Acoustical and optical waveguides are fabricated using Ti(titanium) in-diffusion technology. In a first step the acoustical waveguides are defined by a diffusion (24 hrs at 1050 °C) of a 1,600 Å thick Ti-layer into the cladding region of the acoustical guiding structures, which are 20 mm long tapered acoustical directional couplers. This diffusion technique for producing acoustic velocity perturbation on the order of 1% is suitable for fabricating low-loss acoustic waveguides, which allow a lateral confinement of SAWs.

Subsequently, the optical waveguides structure is fabricated again by Ti in-diffusion (8 hrs at 1050 °C). For single mode waveguides about 1,000 Å thick, 8 μm wide Ti stripes have been diffused. To suppress Li out-diffusion, the diffusion has been performed in wet  $\text{O}_2$  ambient [11].

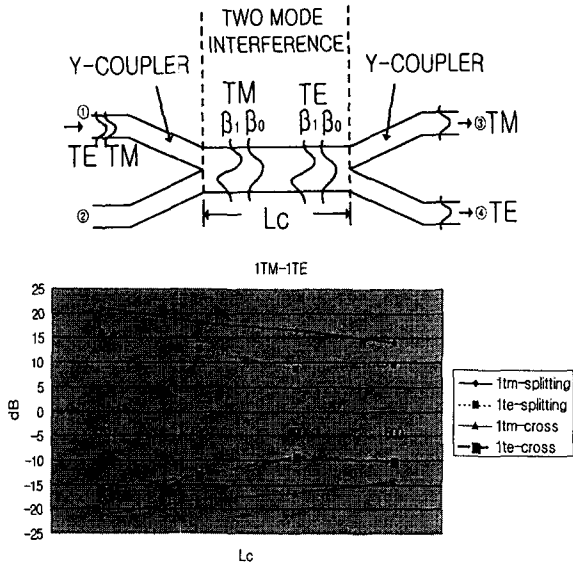


FIG. 2. Design layout of polarization splitter based on the two-mode interference, and measured splitting ratio and cross-talk for TE and TM polarizations versus interference length  $L_c$ .

The insertion loss of the optical waveguides with input port 1 has been measured to be about -8.16 dB and -8.6 dB for TE and TM polarizations, respectively.

## 2. Polarization Splitter

The principle of operation of the polarization splitter is based on two-mode interference in an optical directional coupler. Its schematical diagram is shown in Fig. 2. The two incoming single-mode optical waveguide combine to a double-mode waveguide of twice the width (namely, zero-gap coupler). Within the structure the accumulated phase difference  $\Delta\Phi$  between the interfering symmetrical, fundamental and the asymmetrical, first-order modes results in a beating of the optical power density. The output power will be localized in either branch if this phase difference is a multiple of  $\pi$ . Therefore, the structure operates as a polarization splitter, if  $\Delta\Phi$  is an even multiple of  $\pi$  for one polarization and an odd one for the other. This can be achieved by a careful design [12].

The measured splitting ratios, defined by the ratio of the power in the unwanted output port and the total output power, for TE and TM polarizations, are shown as a function of the central section length  $L_c$  as shown in Fig 2. The splitting ratio with waveguide width  $8\ \mu\text{m}$ , branching angle  $0.55^\circ$  and interfering length  $470\ \mu\text{m}$  shows 16.18 dB and 21.25 dB for TE and TM input polarization mode, respectively. Also, cross-talk of -16.28 dB and -21.28 dB for TE and TM mode have been achieved. The BPM-CAD simulation results of optical wave propagation of the OADM

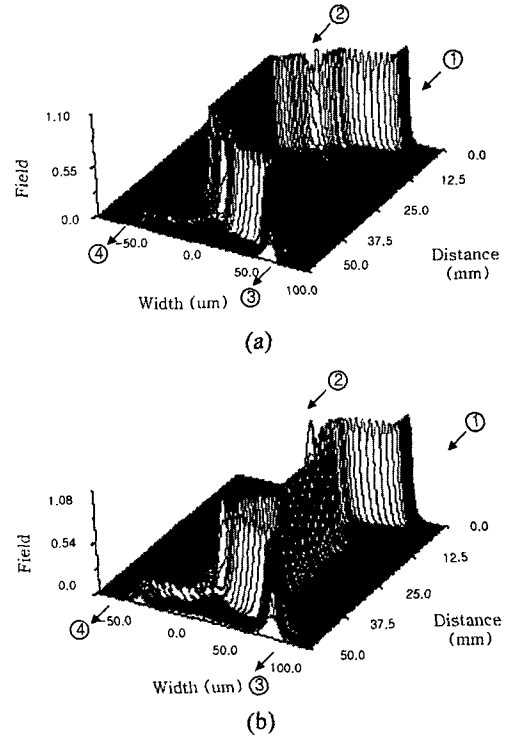


FIG. 3. Optical field distribution of the OADM simulated by BPM-CAD for (a) TE input mode and (b) TM input mode.

consisting of two polarization splitters with branching angle  $0.55^\circ$  and interfering length  $470\ \mu\text{m}$ , and  $8\ \mu\text{m}$  width optical channel waveguides are shown in Fig. 3. It is clearly seen that polarization-independent operation of the device follows from the recombination of both TE and TM components in same channel waveguide (input port 1  $\rightarrow$  output port 3) regardless of state of polarization.

## IV. ACOUSTO-OPTICAL MODE CONVERTERS WITH WEIGHTED COUPLING

The acousto-optical mode converters studied here utilize a tapered acoustical directional coupler structure as shown in Fig. 4. The directional coupler is formed by  $110\ \mu\text{m}$  wide acoustical waveguides. One of these guides is straight whereas the other one is inclined in the outer sections by an angle of  $0.6^\circ$ , resulting in a linear change of the gap between  $70\ \mu\text{m}$  and  $0\ \mu\text{m}$ . In the straight acoustical guide the optical waveguide is embedded. In the other arm the SAW is excited via an RF signal applied to the IDT electrode. suppression down to about -15 dB has been achieved.

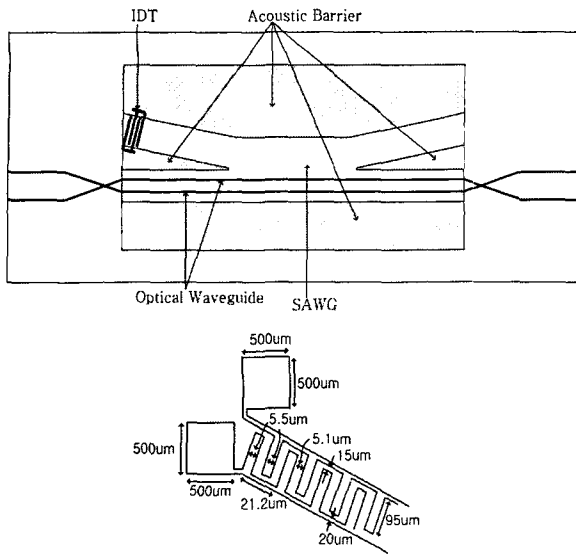


FIG. 4. Design layout of integrated 2 × 2 optical add/drop multiplexer with a tapered acoustic directional coupler, and inter-digital transducer electrode.

A detailed analysis of the acousto-optical mode conversion within acoustical directional couplers is given in [13].

The SAW's are excited via aluminium (~3000 Å) inter-digital transducer electrodes consisting of 20 fingers pairs with a period 21.2 μm. Scotch tapes acting as acoustical absorbers are used to terminate the acousto-optical interaction length. Fig. 5 is the microscope surface photograph of fabricated OADM with IDT electrode.

V. EXPERIMENTAL RESULTS

The OADM has been first characterized by either

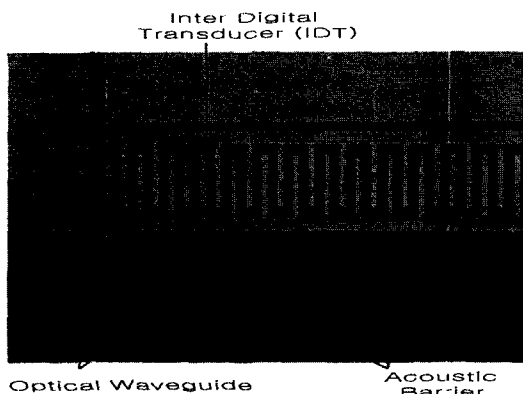


FIG. 5. The microscope surface photograph of fabricated OADM with IDT electrode.

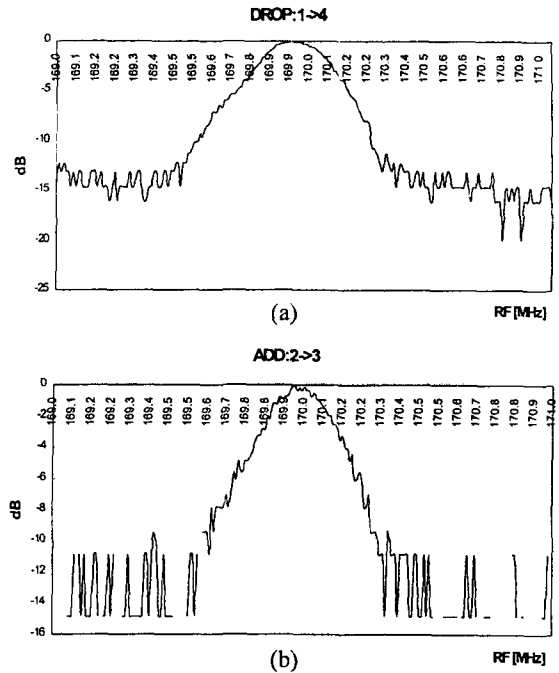


FIG. 6. Switching(drop) characteristics of the OADM for random polarization. The diagram shows the transmission of (a) 1 → 4 and (b) 2 → 3 versus the SAW frequency at fixed optical wavelength, 1554 nm.

varying the acoustic frequency at a fixed optical wavelength using a DFB laser diode at λ = 1554 nm. In Fig. 6, the measured switching characteristics versus the SAW frequency for random polarization are shown. The frequency for the SAW has been adjusted to yield this maximum conversion at the wavelength. Figs. 6(a) and (b) show the transmission (namely, drop) of 1 → 4 and 2 → 3 versus the SAW frequency, respectively. The largest sidelobe occurring on the high frequency side of the transmission curve is about 13 dB below the maximum transmission as shown in Fig. 6(a). Theoretically, a sidelobe suppression of more than about 24 dB is expected [9]. This deviation is due to inhomogeneities mainly of the optical waveguides along the interaction length resulting in a locally varying birefringence and therefore, in a variation of the phase-match frequency.

We have measured the transmission characteristics of the devices by coupling random polarized light from a broadband amplified spontaneous emission (ASE) of an erbium doped fiber amplifier into the input ports or , thereby passing the converter through the outer or inner waveguide, respectively. The SAW frequency has been adjusted to yield polarization conversion and thereby switching at λ = 1547.9 nm. The results of these measurements are shown in Figs. 7 and 8. In the cross-state transmission spectra (1 → 4, 2 → 3) sidelobes about 14.5 dB below the maximum level

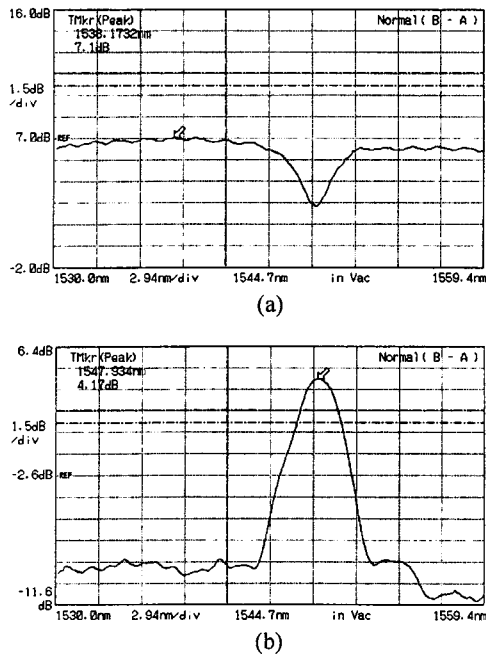


FIG. 7. Switching characteristics of the OADM with a SAW frequency of 171 MHz. The diagrams show the transmission for random polarization versus optical wavelength into the (a) bar-state (1 → 3) and (b) cross-state (1 → 4) for input port 1.

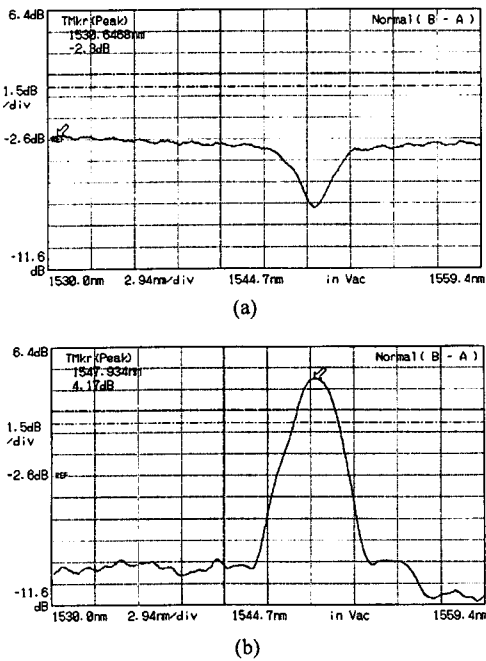


FIG. 8. Switching characteristics of the OADM with a SAW frequency of 171 MHz. The diagrams show the transmission for random polarization versus optical wavelength into the (a) bar-state (1 → 4) and (b) cross-state (2 → 3) for input port 2.

occur at the longer wavelength side that is mainly due to inhomogeneities of the optical waveguides. The total electrical RF power required to drive the switch is about 43 mW. Full-width at half maximum of the transmission curve is about 3 nm.

The relative large sidelobe can again be explained by remaining inhomogeneities in the structure. Moreover, the situation for this OADM is more complex. The polarization splitters typically have an extinction ratio of 16 ~ 20 dB. Therefore, a small fraction of the in-coupled wave is routed the "wrong" way through the device. This may contribute as well to some deviations from the theory.

In a WDM system, the cross-talk from neighboring wavelengths depends on the wavelength channel separation. To demonstrate the multi-wavelength switching capability of the device it has been driven with two RF signals simultaneously switching two wavelengths 8 nm apart. In Fig. 9, the spectral dependencies of the transmission into the cross-states from input port 1 are shown for random input polarization and a wavelength channel spacing of 8 nm. The device has been driven by two RF signals at 170.52 MHz and 171.5 MHz simultaneously. In this case, an extinction ratio of 10 dB is achieved in the cross-state output. When reducing the channel spacing to 4 nm the extinction ratio in the bar-state output decreases due to inter-channel interaction and the cross-state output transmission spectrum shows a significant overlap of the transmission spectra of both channels.

By the way, the maximum transmission at both wavelengths can be adjusted separately by controlling the power levels of the corresponding RF drive frequencies. Therefore, an acousto-optical filter can be used as power or gain EDFA equalizer in a WDM network. It simultaneously suppresses unwanted noise generated by the polarization of broadband EDFA.

Tuning of the switch is measured by varying the acoustic frequency as shown in Fig. 10. The tuning

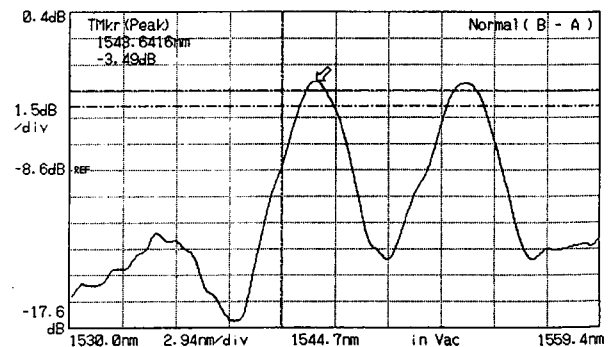


FIG. 9. Simultaneous two-wavelength operation with SAW frequencies of 170.52 and 171.5 MHz. The separation of channels is about 8 nm.

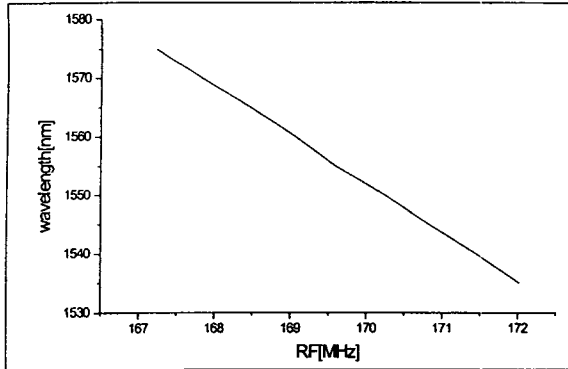


FIG. 10. Measured tuning characteristics of the OADM. Tuning rate is about  $-8.34$  nm/MHz.

slope is given by  $-8.34$  nm/MHz. The tuning range is mainly determined by the bandwidth of the transducers.

## VI. CONCLUSION

We have developed integrated optical  $2 \times 2$  add/drop multiplexers in  $\text{LiNbO}_3$ . A filter bandwidth of 3 nm and a tuning rate of  $-8.34$  nm/MHz have been achieved. The insertion loss of the optical waveguides has been measured to be about  $-8.16$  dB and  $-8.6$  dB for TE and TM polarizations, respectively. Sidelobe suppression is larger than 14.5 dB. At  $\lambda = 1548$  nm an electrical drive power of only 43 mW is required.

The observed incomplete switching and extinction can be improved by optimizing the efficiency of the polarization splitter and mode converter sections. The performance of the switches can be further improved by implementation of acousto-optical mode converters with flat-top conversion characteristics. This will

make the devices less sensitive to fabrication tolerances as well as temperature and laser wavelength drifts.

## ACKNOWLEDGEMENT

This work is partially supported by the basic research fund (2000-1-30200-010-3) of Korea Research Foundation, South Korea.

\*Corresponding author : hsjung@wow.hongik.ac.kr.

## REFERENCES

- [1] Terumi Chikama, Hiroshi Onaka, and Satoshi Kuroyanagi, *Fusitsu Sci. Tech. J.* **35-1**, 46 (1999).
- [2] S. Rotolo *et al.*, *J. Lightwave Technol.* **18**, 569 (2000).
- [3] A. Jourdan *et al.*, *J. Lightwave Technol.* **14**, 1198 (1996).
- [4] J. L. Jackel *et al.*, *J. Lightwave Technol.* **14**, 1056 (1996).
- [5] W. Warzanskyj, F. Heismann, and R. C. Alferness, *Appl. Phys. Lett.* **53**, 13 (1988).
- [6] Z. Tang, O. Eknayan, and H. F. Taylor, *Electron. Lett.* **30**, 1758 (1994).
- [7] F. Wehrman *et al.*, *IEEE J. Selective Topics in Quantum Electron.* **2**, 263 (1996).
- [8] H. Herrmann, U. Rust, and K. Schafer, *J. Lightwave Technol.* **13**, 364 (1995).
- [9] A. K.-Roy and Ch. S. Tsai, **30**, 1574 (1994).
- [10] K.-H. Lim and H.-S. Jung, *J. the Optical Society of Korea* **11**, 193 (2000).
- [11] K.-H. Lim and H.-S. Jung, *J. the Optical Society of Korea* **11**, 423 (2000).
- [12] A. Neyer, *Appl. Phys. Lett.* **55**, 927 (1989).
- [13] G.-J. Jung, J.-H. Kim, and H.-S. Jung, *J. the Institute of Electronics Engineers of Korea* **39-D**, 58 (2002).